NIH Public Access
Author Manuscript
*Ophthalmic Genet*. Author manuscript; available in PMC 2013 May 16.

Published in final edited form as:
*Ophthalmic Genet*. 2009 December ; 30(4): 172–180. doi:10.3109/13816810903176765.

# Retinal Pathology of a Patient with Goldmann-Favre Syndrome

**Vera L. Bonilha, PhD**[1], **Gerald A. Fishman, MD**[2], **Mary E. Rayborn, MS**[1], and **Joe G. Hollyfield, PhD**[1]

[1]The Cole Eye Institute, The Cleveland Clinic Foundation, Cleveland, OH, USA, P:216-445-3252, F:216-445-3670

[2]Department of Ophthalmology and Visual Sciences, University of Illinois, Chicago, IL, USA, P: 312-996-8938, F:312-996-1950

## Abstract

**Purpose—**To define the retinal pathology in an 88 year-old male affected with Goldmann-Favre syndrome with a 2bp 5′ A>C splice site mutation in the NR2E3 gene.

**Methods—**Retinal tissue from the macula and periphery was processed for immunohistochemistry. Perimacular retina was processed for transmission electron microscopy. Cryosections were studied by indirect immunofluorescence, using well-characterized antibodies to rhodopsin, cone cytoplasm, and cone opsins. The affected donor eye was compared to a postmortem matched normal eye.

**Results—**The retina was highly disorganized without laminar organization. The RPE was discontinuous in some perimacular regions. Large (>1mm) spherical electrondense melanosomes were observed in the RPE and choroid by TEM. Rods were virtually absent in the affected retina. Cones were present in the macula, but were mostly absent from the retinal periphery. In addition, cone rosettes were observed in the perimacular area. Both red/green and blue cone opsins were distributed along the entire cellular expanse of the cone photoreceptors in the affected eye, but were restricted to the cone outer segments in the control retina.

**Conclusions—**The histological data obtained from the retina of an elderly male patient with Goldmann-Favre syndrome showed an absence of rods and abnormal distribution of red/green and blue cone opsins.

### Keywords

Goldmann-Favre syndrome; cone opsins; histology; immunohistochemistry; pigment clumping; retinal degeneration; rhodopsin

## Introduction

The Goldmann-Favre syndrome (GFS) is an autosomal recessive distinctive vitreoretinal degenerative disorder initially described in two separate reports in 1957[1] and 1958.[2] GFS is characterized by night blindness, pigmentary degeneration, macular and peripheral retinoschisis, posterior subcapsular cataract, markedly abnormal or nondetectable

Address for reprint requests: Vera L. Bonilha, PhD, Cleveland Clinic Foundation, The Cole Eye Institute, 9500 Euclid Avenue, i31, Cleveland, OH 44195, Phone: 216-445-7690, Fax: 216-445-3670, bonilhav@ccf.org.

The authors have no conflict of interest with the work presented here.

This work was presented at the Association for Research in Vision and Ophthalmology Annual Meeting, May, 2008 and at the XIIIth International Symposium on Retinal Degeneration Meeting, September, 2008 and at XVIII ICER08.

NIH-PA Author Manuscript
NIH-PA Author Manuscript
NIH-PA Author Manuscript

NIH-PA Author Manuscript

NIH-PA Author Manuscript

NIH-PA Author Manuscript

electroretinograms, and degenerative vitreous changes, such as liquefaction, and the presence of strands and/or bands. Since the original description, a number of other cases have been reported confirming that this is a clinically recognizable disease but it is now known that the specific clinical features vary among pedigrees.[3–9]

More recently, it was proposed that the GSF is a phenotypic variant of the enhanced S-cone syndrome, since in both retinal dysfunctions the patients display hypersensitivity to short-wavelength and their electroretinograms have greater amplitudes to short-wavelength (eg, blue) light flashes than to long-wavelength (eg, orange) light flashes.[10]

The GFS is caused by loss-of-function mutations in the *NR2E3* gene (also known as *PNR*). The *NR2E3* gene encodes a retinal nuclear receptor recently discovered to be a ligand-dependent transcription factor[11] specifically found in photoreceptors. Although the morphology and physiology of photoreceptors are well documented, the developmental pathways from a multipotent retinal progenitor to a committed precursor and a terminally-differentiated photoreceptor are only beginning to be elucidated. It is thought that *NR2E3* controls photoreceptor differentiation by repressing the expression of cone-specific genes in rods.[12, 13] However, it is not known how the mutation in this gene leads to the degeneration of the RPE and retina.

Previously, a histopathological analysis from a full-thickness eye-wall biopsy of the eye of a young patient affected by GFS was reported.[5] In the present study we analyzed the morphology of the retina and the distribution of photoreceptor markers in a donor eye from a male donor affected by GFS. To our knowledge this is the first immunohistological study performed in a GFS affected eye.

## Materials and Methods

### Patient information

The donor was an 88 year-old man who died from congestive heart failure. He was an affected member of a family with autosomal recessive Goldmann-Favre syndrome. The eyes were obtained through the National Retinitis Pigmentosa Foundation Donor Program (donation number #816). The donor had an ocular exam one year prior to his death.

The clinical evaluation of the patient was carried out at the University of Illinois with the approval of the Institutional Review Board (IRB) at the University of Illinois Medical Center. However, since this is a single case report, IRB approval was not needed for this project.

### Histopathology

The immunocytochemistry analysis was performed at the Cleveland Clinic, where use of human tissues obtained and used after deceased is exempt from IRB approval. The donor globes were fixed 12 hrs post-mortem in a mixture of 4% paraformaldehyde and 0.5% glutaraldehyde made in 0.1M phosphate buffer, pH 7.3. After 1 month in fixative, the globes were transferred and stored in 2% paraformaldehyde prepared in the same buffer. The eyes from a 78 year-old male and a 91 year-old male were used as controls, and were fixed 4.5 hr and 8.5 hr post-mortem in 2% paraformaldehyde made in the same buffer. Tissue from the macula and periphery were cut, and the tissue was infused successively with 10% and 20% sucrose in PBS, and embedded in Tissue-Tek “4583” (Miles Inc., Elkhart, IN). Ten μm cryosections were cut on a cryostat HM 505E (Microm, Walldorf, Germany) equipped with a CryoJane Tape-Transfer system (Instrumedics, Inc., Hackensack, NJ).

NIH-PA Author Manuscript

NIH-PA Author Manuscript

NIH-PA Author Manuscript

Prior to labeling, embedding medium was removed through two consecutive PBS incubations for 20 min. The tissue was then processed for immunofluorescence labeling as previously described.[14] Briefly, tissues were blocked in PBS supplemented with 1% BSA (PBS/BSA) for 30 min and incubated with the antibodies in PBS/BSA overnight at 4°C. Cryosections of both the matched control and affected donor tissues were labeled with the following antibodies: rabbit polyclonal antibody AB5407 to blue cone opsin (1: 1200, Chemicon International, Inc., Temecula, CA), rabbit polyclonal antibody AB5405 to red/green cone opsins (1: 1200, Chemicon International, Inc., Temecula, CA), monoclonal antibody B6-30N to rhodopsin (1:50, from Dr. P. Hargrave, University of Florida, Gainesville, FL, U.S.A.), and the monoclonal antibody 7G6 to cone arrestin (1:100, from Dr. P. MacLeish, Morehouse School of Medicine, Atlanta, GA)[15]. Cell nuclei were labeled with TO-PRO®-3 iodide (1mg/ml, Molecular Probes, Eugene, OR). Secondary antibodies (goat anti-mouse or anti-rabbit IgG; 1:1000) were labeled with Alexa Fluor 488 (green; Molecular Probes). Sections were analyzed using a Leica laser scanning confocal microscope (TCS-SP2, Leica, Exton, PA). A series of 1 μm *xy* (*en face*) sections were collected. Each individual *xy* image of the retinas stained represents a three-dimensional projection of the entire cryosection (sum of all images in the stack). Microscopic panels were composed using AdobePhotoshop CS3 (Adobe, San Jose, CA).

### Ultrastructural analysis

A small area of the retina/RPE/choroid tissue from the perimacula region of the affected donor and matched-controls (78 and 91 year-old males with 4.5 and 7.5 hr post-mortem) were fixed in 2.5% glutaraldehyde and 0.1M cacodylate buffer, sequentially dehydrated in ethanol and embedded in Epon as previously reported.[16] One μm plastic sections of both samples were stained with toluidine blue and examined and photographed by light microscopy with a Zeiss Axiophot microcroscope (Zeiss). equipped with a Hamamatsu C5810 camera. Thin sections were prepared and electron micrographs were taken on a Tecnai 20 200 kV digital electron microscope (Philips, Hillsboro, OR) using a Gatan image filter and digital camera at 3600 diameters and were printed at identical magnifications.

## Results

### Clinical Findings

The patient was initially seen at age 57 years with a history of poor night vision for as long as he could remember. He also complained of blurred central vision and impairment of his peripheral visual field. His family pedigree showed that of five siblings, a deceased sister was known to have had poor vision from an early age.

He was last seen for a follow-up eye examination in February, 2006 at 87 years of age which was one year prior to his death. At that time, his visual acuity was correctable to 20/400 in the right eye and 20/200 in the left. The corneas were clear and he had bilateral posterior capsule intraocular lens implants. Ocular pressures by applanation were 15 mmHg in each eye.

His retinal examination showed atrophic-appearing changes in the macula of each eye. The retinal vessels were attenuated and the optic disc in each eye showed a “waxy”-appearing atrophy. The peripheral retina showed extensive pigment clumping, which was spherical in appearance and present for 360°. Predominantly in the inferotemporal quadrant, there was a peripheral retinoschisis in each eye. Goldmann kinetic visual fields obtained four years prior to his death showed severe concentric restriction to even a large V4e test target in each eye.

A 2bp 5′ A>C splice site mutation in the NR2E3 gene had been previously identified.

NIH-PA Author Manuscript

NIH-PA Author Manuscript

NIH-PA Author Manuscript

**Morphologic Study—**Semi-thin sections of epon-embedded GFS donor tissue were analyzed and compared to age-similar controls (Figure 1). The fundus image of the posterior pole of the GFS **patient** is depicted in Figure 1A, highlighting hyperpigmentation (white arrowheads) and peripheral retinoschisis (white *) (A); both periphery and perimacular tissues were harvested and processed for observation in both the morphological and ultrastructural assays. The retina of the GFS affected donor displayed different degrees of retinal degeneration in each of the regions observed when compared to the morphology of the control retina in the perimacular (Figure 1B) region of the eye. Observation at low magnification of both perimacula (Figure 1C) and periphery tissue (Figure 1E) demonstrated sparse inner and outer nuclear layers with stunted photoreceptor inner and outer segments. A thin, restricted area of pigmented RPE cells was observed in the perimacular retina (Figure 1, C and D, arrows) while a continuous layer of pigmented RPE cells was observed in the periphery (Figure 1E) of the affected donor. High magnification observation of the affected retina in the periphery (Figure 1F, arrowheads) but not in the perimacular region (Figure 1D) showed the presence of several areas of pigment clumping. In addition, tissue from the inferotemporal quadrant was also evaluated (Figure 1, G and H). This region contained a prominent pre-retina (epiretinal) membrane composed of a monolayer of fibroblast-like cells that were separated from the retina by a connective tissue-like matrix that was free of cells (Figure 1, H and G, *). The separation of this membrane from the retinal surface varied from 10 to 40μm. This membrane was not observed in the other areas of the retina examined.

**Immunofluorescence Study—**To further understand some of the molecular changes associated with the GFS phenotype in this affected donor, tissue from the periphery and macula of his right eye was processed for cryosectioning and immunofluorescence. Initially, the distribution of rhodopsin was analyzed in both the symptomatic carrier and a matched-control eye (Figure 2, A–D). Rhodopsin was absent in both the periphery (Figure 2B) and perimacular (Figure 2, C and D) area of the GFS affected retina. This observation was in sharp contrast to the presence of rhodopsin in the outer segments observed in the control retina (Figure 2A).

In addition, cryosections were also labeled with cone specific markers. Initially, the distribution of the cone cytoplasmic marker 7G6 was analyzed in both the GFS affected donor and a matched-control eye (Figure 3, A–D). In the GFS affected retina, a complete absence of cones was observed in the periphery (Figure 3B). However, in the perimacular area, a high density of cones (Figure 3C) was observed together with the presence of several rosettes (Figure 3D). In contrast to cones in the control sample (Figure 3A), the cones in the GFS affected retina did not display a synaptic base (Figure 3, B–D). Moreover, cell nuclei, labeled with TO-PRO-3, displayed a significant difference in the organization of the all retinal cell types when compared to the matched control.

Additional characterization of the GFS affected donor also included the labeling of this retina with antibodies directed to red/green cone opsin. The control retina displayed the red/green cone opsin restricted to its outer segments (Figure 4A). However, a striking abnormal distribution of the red/green opsins throughout the entire cone cell body was observed in the perimacular regions of the affected retina (Figure 4C); the abnormal distribution was also observed in rosettes within the perimacular region (Figure 4D). On the other hand, red/green opsins were mostly absent in the periphery of the affected retina (Figure 4B).

Both a matched control and affected GFS donor eyes were labeled with antibodies specific to blue cone opsins (Figure 5). The control retina displayed the blue cone opsin restricted to its outer segments (Figure 5A). However, a significant increase in blue cone opsin was observed in all regions of the cone structure in the GFS affected eye (Figure 5, B–D) where

NIH-PA Author Manuscript

NIH-PA Author Manuscript

NIH-PA Author Manuscript

the blue cone opsin was distributed along the entire plasma membrane of this cone type; the abnormal distribution was also observed in rosettes in the perimacular region (Figure 5D).

### Ultrastructural pathology

The ultrastructure of RPE and Bruch's membrane in the perimacula tissue was analyzed by TEM (Figure 6). Observation at both low (Figure 6, B and C) and high (Figure 6D) magnification showed a collapsed RPE apical surface mostly deprived of apical microvilli; no photoreceptor outer segments were observed anterior to the RPE apical surface. Moreover, observation of the RPE's basal surface showed an absence of basal infoldings (Figure 6D, arrows); Bruch's membrane was notably disorganized (Figure 6, B and C) when compared to control sample (Figure 6A). Some areas displayed multilayers of pigmented cells (Figure 6C). Interestingly, the presence of desmosomes (Figure 6, C and D, arrowheads) was noticed between adjacent cells. The cytoplasm of RPE cells was filled with abnormally large (>1mm) spherical electrondense melanosomes (Figure 6, B and C) when compared to control RPE cells (Figure 6A).

## Discussion

Histopathological analysis of the GFS affected retina showed the presence of different degrees of photoreceptor cell degeneration in both the peripheral and perimacular regions. In this affected donor, RPE degeneration was also observed and documented.

Differentiation of the vertebrate retina is guided by complex interactions between intrinsic genetic programs and extrinsic regulatory factors, entailing precise coordination between withdrawal from the cell cycle and differentiation.[17–21] Acquisition of functional specificity depends on precise spatially and temporally gene expression patterns that are in turn dictated by complex transcriptional regulatory networks.[22–24] In the mammalian retina rod and cone photoreceptors are generated from common pool(s) of neuroepithelial progenitors. Cone-rod homeobox (CRX), neural retina leucine zipper (NRL) and rod-specific orphan nuclear receptor (NR2E3) are key transcriptional regulators that control photoreceptor differentiation.[25–27, 11]

Enhanced S cone syndrome (ESCS) patients, as well as patients with Goldman-Favre syndrome and some patients with clumped pigmentary retinal degeneration, carry mutations in the NR2E3 gene. Specifically, loss-of-function mutations in this gene cause a disorder of human retinal photoreceptor development characterized by hyperfunction and excess of the normally minority S (short wavelength or blue) cone photoreceptor type together with near absence of function of the majority of rod receptors.[28, 12, 29–31] Moreover, multiple mutations in the mouse Nr2e3 gene were identified in the rd7 mouse model.[32, 33] The rd7 mice exhibit a progressive rod degeneration accompanied by 1.5–2 fold increase in the number of S-cones.[32–34]

The human retina is composed of roughly 90% red/green and 10% blue cones.[35–37] However, the data obtained in the analysis of the GFS affected retina revealed a significant increase in blue cone opsins both in the periphery and perimacular region. A high proportion of rods over cones (over 95%) also characterize the normal human retina. The GFS affected retina was characterized by an almost complete absence of rods. The photoreceptor phenotypes described above are in agreement with the previously described Nr2e3 mutations in humans and rodents, which led to excess of the minority of the S (short-wavelength or blue) cone photoreceptor type together with near absence of rod function.

In the present case, a striking cone abnormality was the presence of both red/green and blue opsins throughout the entire cone cell body instead of the usual restriction to the outer

NIH-PA Author Manuscript

NIH-PA Author Manuscript

NIH-PA Author Manuscript

segment. A previous study of enhanced S-cone syndrome donor eyes reported the presence of abnormal distribution of both S- (blue) and L/M-(red/green) cone opsins along the entire plasma membranes of the cells, including their inner segments, cell bodies, axon and pedicles.[28] More recently, an affected member of a clinically well characterized family with an autosomal dominant form of cone dystrophy was also shown to exhibit distribution of the red/green cone opsin from the tip of the outer segment to the pedicle.[35] Moreover, a recent retinitis pigmentosa GTPase regulator (RPGR)-deficient murine model was also shown to have initial ectopic or unrestricted distribution of both red/green and blue opsins and a reduced level of rhodopsin followed by the subsequent degeneration of cones and rods.[38] That report suggested that mislocalization of cone opsins may precede cone cell death. Finaly, a recent report described red/green opsin distribution throughout the cell membrane of the heterozygous P23H-3 rhodopsin rat transgenic retinas from postnatal day 16 to 500.[39]

Another unique phenotype of the GFS affected retina was the presence of rosettes of both red/green and blue cone opsin in the perimacular region. The rd7 mouse model is characterized histologically by retinal dysplasia manifesting as folds and whorls labeled with blue cone opsin antibody in the photoreceptor layer.[33] The authors that described the retinal dysplasia speculated that Nr2e3 might function by regulating genes involved in cone cell proliferation. Further studies will be necessary to unravel the function of Nr2e3 in the generation of retinal folds or rosettes.

The processing of visual information from the environment begins at the output of the photoreceptor synapse with neurons in the inner layers of the retina. No cone pedicles were observed in the GFS affected retina when labeled with the cone arrestin antibody, in contrast to what was observed in control retinas. Therefore, it is possible that the GFS affected retina could not effectively process visual information.

In the GFS affected retina, the RPE cells were significantly different from control matched RPE cells. A thin, restricted area of pigmented RPE cells was observed in the perimacular retina while a continuous layer of pigmented RPE cells was observed in the periphery; these pigmentary changes are likely associated with the clinical clumped pigmentary retinal findings frequently reported in Goldmann-Favre patients. The ultrastructural observation of the perimacular area revealed a collapsed RPE apical surface mostly deprived of apical microvilli and basal infoldings. Moreover, Bruch's membrane was extensively disorganized. Some areas displayed multilayers of pigmented cells where the presence of desmosomes was noticed between adjacent cells. The cytoplasm of RPE and choroidal cells was filled with abnormally large (>1mm) spherical electrondense melanosomes. Further analysis of these melanosomes is needed for a better understanding of their role in the pathologic changes observed. A previous histopathologic analysis of a full-thickness eye-wall biopsy obtained from the eye of a young patient with Goldmann-Favre syndrome, from a 4 mm peripheral area, displayed diffuse degenerative changes involving predominantly the sensory retinal layers with a relatively normal pigment epithelium and choroid.[5]

In conclusion, we report here the clinical findings and abnormal distribution of the red/green and blue cone opsins throughout the entire cone cell bodies together with absence of rhodopsin in the retina from a donor diagnosed with GFS. The red/green and blue cones were also observed in rosettes uniquely present in the perimacular area. These results are important to our understanding of one of possibly several molecular mechanisms underlying this disease. It also suggests that vision loss in this patient may result not only from abnormal Nr2e3 but also from secondary neuronal death and corrupted retinal circuitry due to the irreversible effects of retinal remodeling.

NIH-PA Author Manuscript

NIH-PA Author Manuscript

NIH-PA Author Manuscript

## Acknowledgments

The authors thank Dr. Peter MacLeish (Morehouse School of Medicine, Atlanta, GA) for providing us with the antibody to cone arrestin (7G6), Dr. Paul Hargrave (University of Florida, Gainesville, FL) for providing us with the antibody to rhodopsin (B6-30N). This work was supported by The Foundation Fighting Blindness, Owings Mills, MD, NIH infrastructure grant EY015638 and an unrestricted grant from Research to Prevent Blindness.

## References

1. Goldmann H. Prèsentation du rapport sur la biomicroscopie du du corps vitrè et du fond d'oeil. Bull Mem Soc Fr Ophtalmol. 1957; 70:265–272.
2. Favre M. Two cases of hyaloid-retinal degeneration. Ophthalmologica. 1958; 135:604–609. [PubMed: 13553271]
3. Fishman GA, Jampol LM, Goldberg MF. Diagnostic features of the Favre-Goldmann syndrome. Br J Ophthalmol. 1976; 60:345–353. [PubMed: 1085161]
4. Schmidt B, Weinberg M. Atypical retinopathia pigmentosa with central retinoschisis (Goldmann-Favre). Klin Monatsbl Augenheilkd. 1976; 169:508–512. [PubMed: 1086927]
5. Peyman GA, Fishman GA, Sanders DR, Vlchek J. Histopathology of Goldmann-Favre syndrome obtained by full-thickness eye-wall biopsy. Ann Ophthalmol. 1977; 9:479–484. [PubMed: 301373]
6. Izumi K, Matsuhashi M. Goldmann-Favre syndrome in a four-year-old-girl. Doc Ophthalmol. 1987; 66:219–226. [PubMed: 3428076]
7. Nasr YG, Cherfan GM, Michels RG, Wilkinson CP. Goldmann-Favre maculopathy. Retina. 1990; 10:178–180. [PubMed: 2236941]
8. Garweg J, Bohnke M, Mangold I. Treatment of Goldmann-Favre syndrome with cyclosporin A and bromocriptine. Klin Monatsbl Augenheilkd. 1991; 199:199–205. [PubMed: 1753674]
9. Ikaheimo K, Tuppurainen K, Mantyjarvi M. Clinical features of Goldmann-Favre syndrome. Acta Ophthalmol Scand. 1999; 77:459–461. [PubMed: 10463423]
10. Jacobson SG, Roman AJ, Roman MI, Gass JDM, Parker JA. Relatively enhanced S cone function in the Goldmann-Favre syndrome. Am J Ophthalmol. 1991; 111:446–453. [PubMed: 2012146]
11. Kobayashi M, Takezawa S, Hara K, Yu RT, Umesono Y, Agata K, Taniwaki M, Yasuda K, Umesono K. Identification of a photoreceptor cell-specific nuclear receptor. Proc Natl Acad Sci U S A. 1999; 96:4814–4819. [PubMed: 10220376]
12. Haider NB, Jacobson SG, Cideciyan AV, Swiderski R, Streb LM, Searby C, Beck G, Hockey R, Hanna DB, Gorman S, Duhl D, Carmi R, Bennett J, Weleber RG, Fishman GA, Wright AF, Stone EM, Sheffield VC. Mutation of a nuclear receptor gene, NR2E3, causes enhanced S cone syndrome, a disorder of retinal cell fate. Nat Genet. 2000; 24:127–131. [PubMed: 10655056]
13. Cheng H, Aleman TS, Cideciyan AV, Khanna R, Jacobisn SG, Swaroop A. In vivo function of the orphan nuclear receptor NR2E3 in establishing photoreceptor identity during mammalian retinal development. Hum Mol Genet. 2006; 15:2588–2602. [PubMed: 16868010]
14. Bonilha VL, Hollyfield JG, Grover S, Hollyfield JG. Abnormal distribution of red/green cone opsins in a patient with an autosomal dominant cone dystrophy. Ophthalmic Genet. 2005; 26:69–76. [PubMed: 16020309]
15. Zhang H, Cuenca N, Ivanova T, Church-Kopish J, Frederick JM, MacLeish PR, Baebr W. Identification and light-dependent translocation of a cone-specific antigen, cone arrestin, recognized by monoclonal antibody 7G6. Invest Ophthalmol Vis Sci. 2003; 44:2858–2867. [PubMed: 12824223]
16. Bonilha VL, Trzupek KM, Li Y, et al. Choroideremia: analysis of the retina from a female symptomatic carrier. Ophthalmic Genet. 2008; 29:99–110. [PubMed: 18766988]
17. Ericson J, Morton S, Kawakami A, Roelink H, Jessell TM. Two critical periods of Sonic Hedgehog signaling required for the specification of motor neuron identity. Cell. 1996; 87:661–673. [PubMed: 8929535]
18. Desai AR, McConnell SK. Progressive restriction in fate potential by neural progenitors during cerebral cortical development. Development. 2000; 127:2863–2872. [PubMed: 10851131]

NIH-PA Author Manuscript

NIH-PA Author Manuscript

NIH-PA Author Manuscript


19. Levine EM, Fuhrmann S, Reh TA. Soluble factors and the development of rod photoreceptors. Cell Mol Life Sci. 2000; 57:224–234. [PubMed: 10766019]
20. Dyer MA, Cepko CL. Regulating proliferation during retinal development. Nat Rev Neurosci. 2001; 2:333–342. [PubMed: 11331917]
21. Ohnuma S, Harris WA. Neurogenesis and the cell cycle. Neuron. 2003; 40:199–208. [PubMed: 14556704]
22. Brivanlou AH, Darnell JE Jr. Signal transduction and the control of gene expression. Science. 2002; 295:813–818. [PubMed: 11823631]
23. Marquardt T, Gruss P. Generating neuronal diversity in the retina: one for nearly all. Trends Neurosci. 2002; 25:32–38. [PubMed: 11801336]
24. Levine M, Davidson EH. Gene regulatory networks for development. Proc Natl Acad Sci U S A. 2005; 102:4936–4942. [PubMed: 15788537]
25. Swaroop A, Xu JZ, Pawar H, Jackson A, Skolnick C, Agarwal N. A conserved retina-specific gene encodes a basic motif/leucine zipper domain. Proc Natl Acad Sci U S A. 1992; 89:266–270. [PubMed: 1729696]
26. Chen S, Wang QL, Nie Z, Sun H, Lennon G, Copeland NG, Gilbert DJ, Jenkins NA, Zack DJ. Crx a novel Otx-like paired-homeodomain protein, binds to and transactivates photoreceptor cell-specific genes. Neuron. 1997; 19:1017–1030. [PubMed: 9390516]
27. Furukawa T, Morrow EM, Cepko CL. Crx a novel otx-like homeobox gene, shows photoreceptor-specific expression and regulates photoreceptor differentiation. Cell. 1997; 91:531–541. [PubMed: 9390562]
28. Milam AH, Rose L, Cideciyan AV, Barakat MR, Tang WX, Gupta N, Aleman TS, Wright AF, Stone EM, Sheffield VC, Jacobson SG. The nuclear receptor NR2E3 plays a role in human retinal photoreceptor differentiation and degeneration. Proc Natl Acad Sci U S A. 2002; 99:473–478. Epub 2002 Jan 2. [PubMed: 11773633]
29. Sharon D, Sandberg MA, Caruso RC, Berson EL, Dryja TP. Shared mutations in NR2E3 in enhanced S-cone syndrome, Goldmann-Favre syndrome, and many cases of clumped pigmentary retinal degeneration. Arch Ophthalmol. 2003; 121:1316–1323. [PubMed: 12963616]
30. Wright AF, Reddick AC, Schwartz SB, Ferguson JS, Aleman TS, Kellner U, Jurklies B, Schuster A, Zrenner E, Wissinger B, Lennon A, Shu X, Cideciyan AV, Stone EM, Jacobson SG, Swaroop A. Mutation analysis of NR2E3 and NRL genes in Enhanced S Cone Syndrome. Hum Mutat. 2004; 24:439. [PubMed: 15459973]
31. Jacobson SG, Sumaroka A, Aleman TS, et al. Nuclear receptor NR2E3 gene mutations distort human retinal laminar architecture and cause an unusual degeneration. Hum Mol Genet. 2004; 13:1893–1902. [PubMed: 15229190]
32. Akhmedov NB, Piriev NI, Chang B, Rapoport AL, Hawes NL, Nishina PM, Nusinowitz S, Heckenlively JR, Roderick TH, Kozak CA, Dacinger M, Davisson MT, Farber DB. A deletion in a photoreceptor-specific nuclear receptor mRNA causes retinal degeneration in the rd7 mouse. Proc Natl Acad Sci U S A. 2000; 97:5551–5556. [PubMed: 10805811]
33. Haider NB, Naggert JK, Nishina PM. Excess cone cell proliferation due to lack of a functional NR2E3 causes retinal dysplasia and degeneration in rd7/rd7 mice. Hum Mol Genet. 2001; 10:1619–1626. [PubMed: 11487564]
34. Curcio CA, Allen KA, Sloan KR, Lerea CL, Hurley JB, Klock IB, Milam AH. Distribution and morphology of human cone photoreceptors stained with anti-blue opsin. J Comp Neurol. 1991; 312:610–624. [PubMed: 1722224]
35. Chen J, Rattner A, Nathans J. Effects of L1 retrotransposon insertion on transcript processing, localization and accumulation: lessons from the retinal degeneration 7 mouse and implications for the genomic ecology of L1 elements. Hum Mol Genet. 2006; 15:2146–2156. [PubMed: 16723373]
36. Roorda A, Metha AB, Lennie P, Williams DR. Packing arrangement of the three cone classes in primate retina. Vision Res. 2001; 41:1291–1306. [PubMed: 11322974]
37. Roorda A, Williams DR. The arrangement of the three cone classes in the living human eye. Nature. 1999; 397:520–522. [PubMed: 10028967]

NIH-PA Author Manuscript

NIH-PA Author Manuscript

NIH-PA Author Manuscript

38. Hong DH, Pawlyk BS, Shang J, Sandberg MA, Berson EL, Li T. A retinitis pigmentosa GTPase regulator (RPGR)-deficient mouse model for X-linked retinitis pigmentosa (RP3). Proc Natl Acad Sci U S A. 2000; 97:3649–3654. [PubMed: 10725384]

39. Chrysostomou V, Stone J, Valter K. Life history of cones in the rhodopsin-mutant P23H-3 rat: evidence of long term survival. Invest Ophthalmol Vis Sci. 2008 Epub 2008 Dec 30.

NIH-PA Author Manuscript
NIH-PA Author Manuscript
NIH-PA Author Manuscript



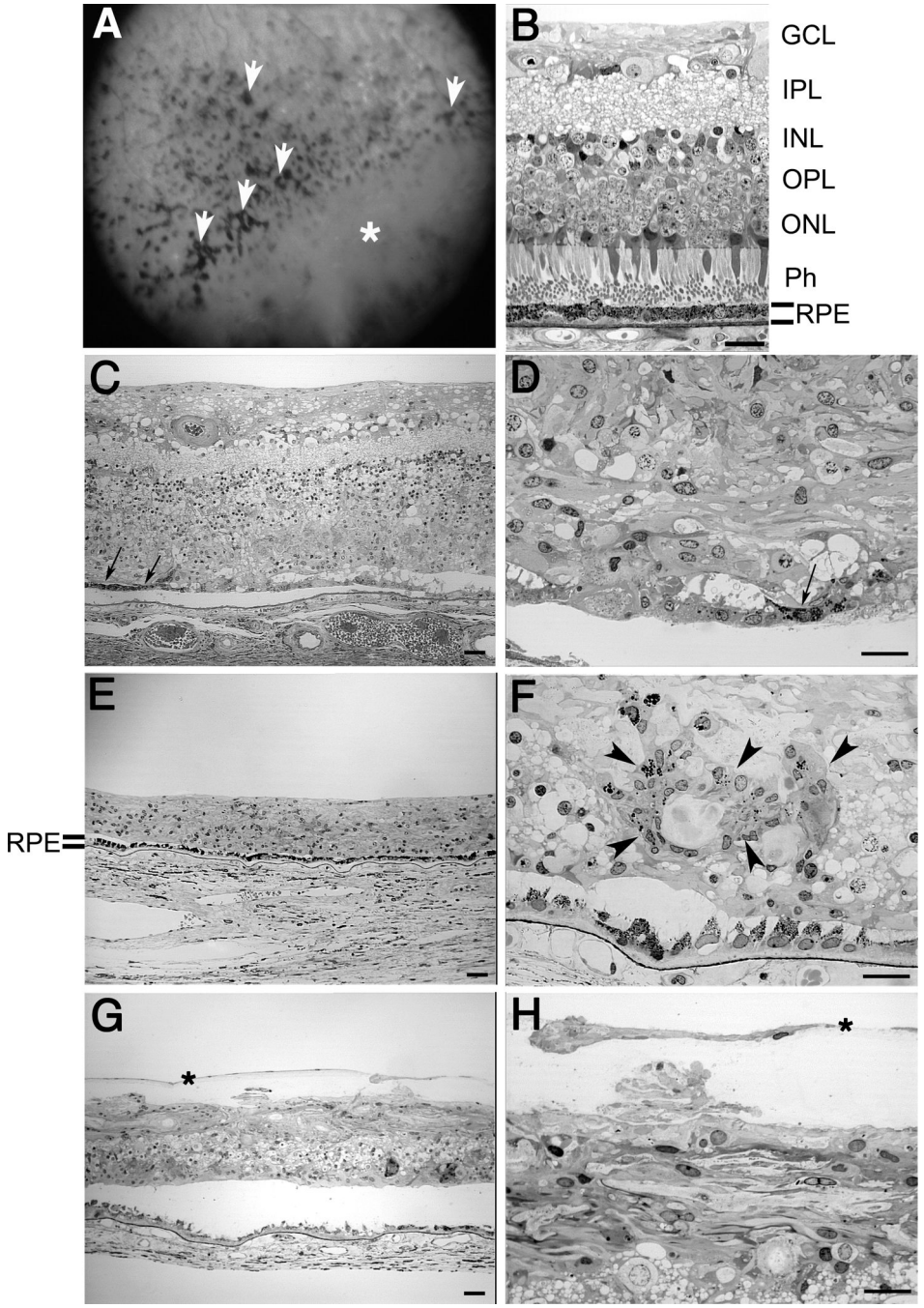


**Fig. 1.**

Degeneration in the retina of a Goldmann-Favre syndrome (GFS) affected donor. Human 1μm plastic sections of both a matched control (B) and the affected GFS (C–F) retinas stained with toluidine blue. Top panel corner depicts a fundus image of the patient's left eye, showing hyperpigmentation (white arrowheads) and peripheral retinoschisis (white *) (A). (B) Morphology of perimacular region of the control eye. (C–F) The retina of the affected GFS donor displayed different degrees of retinal degeneration. Observation at low magnification of both perimacular region (C) and peripheral tissue (E) demonstrated sparse inner and outer nuclear layers with stunted photoreceptor inner and outer segments. A thin, restricted area of pigmented RPE cells was observed in the perimacular retina (C, arrows)

NIH-PA Author Manuscript

NIH-PA Author Manuscript

NIH-PA Author Manuscript

while a continuous layer of pigmented RPE cells was observed in the periphery (E) of the affected donor. High magnification observation of the affected retina in the periphery (F) but not in the perimacular region (D) showed the presence of several clumps of pigment (arrowheads). In addition, tissue from the inferotemporal quadrant was also evaluated (G, H). This region contained a prominent pre-retina (epiretinal) compartment composed of a monolayer of fibroblast-like cells that were separated from the retina by a connective tissue-like matrix that was free of cells (H, G, *). RPE= retinal pigment epithelium; Ph=photoreceptors; ONL= outer nuclear layer; OPL= outer plexiform layer; INL= inner nuclear layer; IPL= inner plexiform layer; GCL= ganglion cell layer. Scale bars C, E, G=40μm; B, D, F, H= 20μm.

NIH-PA Author Manuscript
NIH-PA Author Manuscript
NIH-PA Author Manuscript



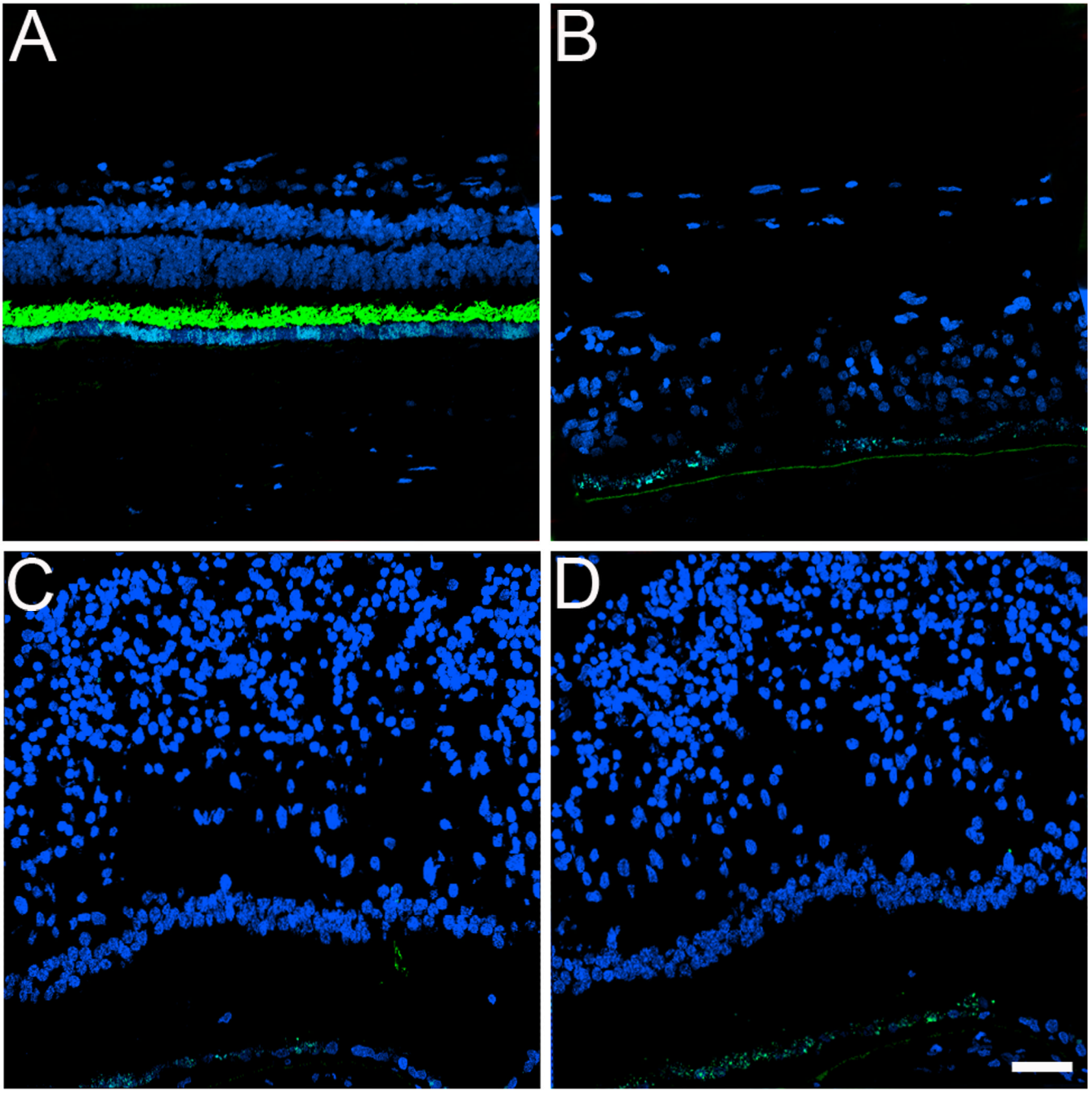


**Fig. 2.**

Absence of rhodopsin in the rods in a GFS affected donor. Human cryosections of both a matched control (A) and affected GFS donor (B–D) were labeled with antibodies specific to rhodopsin (Alexa488, green) while cell nuclei were labeled with TO-PRO-3 (blue). Sections were analyzed using a Leica laser scanning confocal microscope. Comparison of the samples showed that rhodopsin was absent in the affected retina in all the regions observed. Scale bar = 40μm.

NIH-PA Author Manuscript
NIH-PA Author Manuscript
NIH-PA Author Manuscript



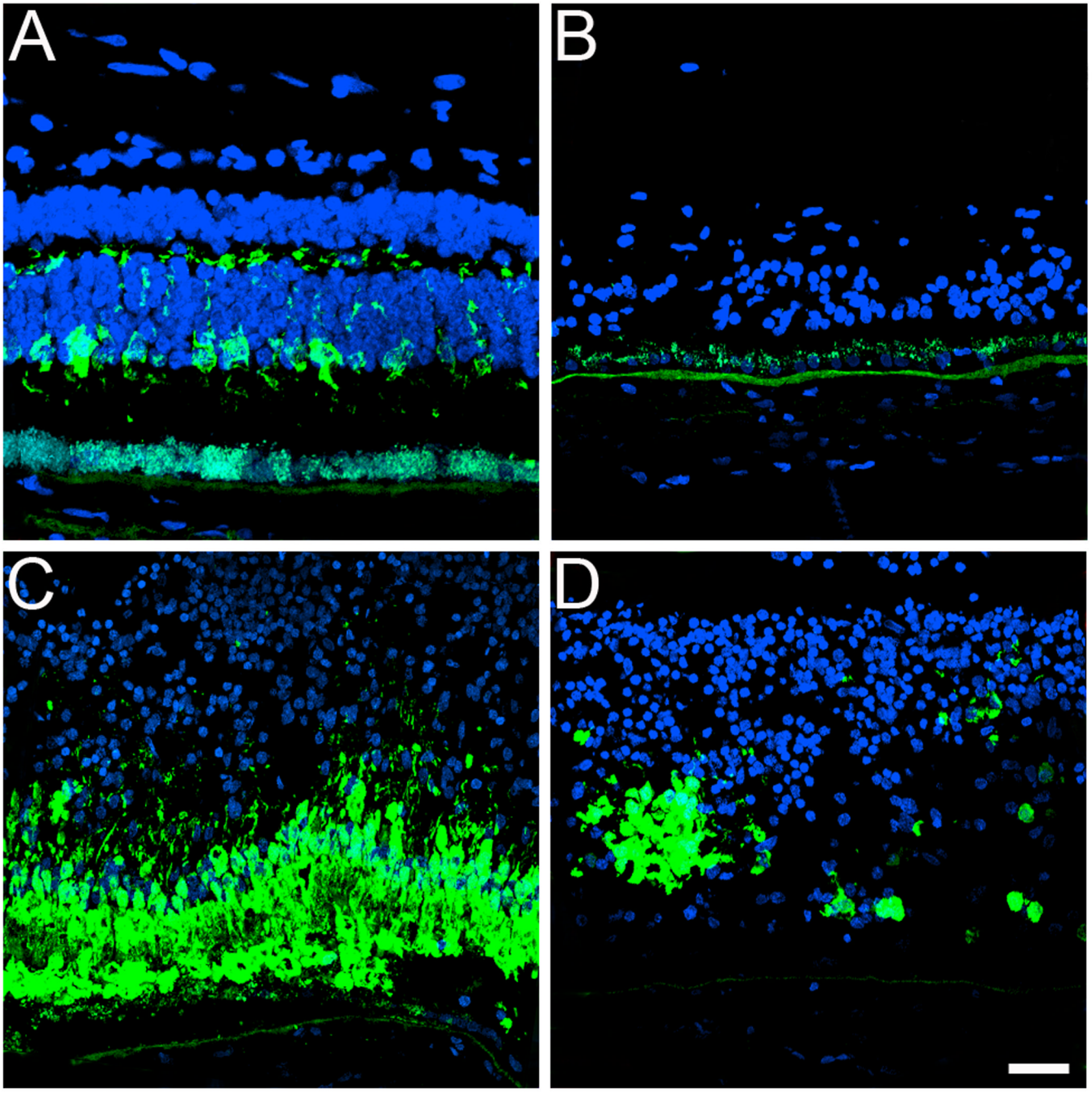


**Fig. 3.**

Significant absence of cones in the periphery together with the presence of rosettes of cones in the perimacular region of a GFS affected donor. Human cryosections of both a matched control (A) and a GFS affected donor (B–D) were labeled with antibodies specific to cone cytoplasm (7G6, Alexa488, green) while cell nuclei were labeled with TO-PRO-3 (blue). Sections were analyzed using a Leica laser scanning confocal microscope. Comparison of the samples showed that cones were almost absent in the periphery (B) while in the perimacular region they were present in high density (C). Cones were also distributed in rosettes in the perimacular region (D). Scale bar = 40μm.

NIH-PA Author Manuscript
NIH-PA Author Manuscript
NIH-PA Author Manuscript



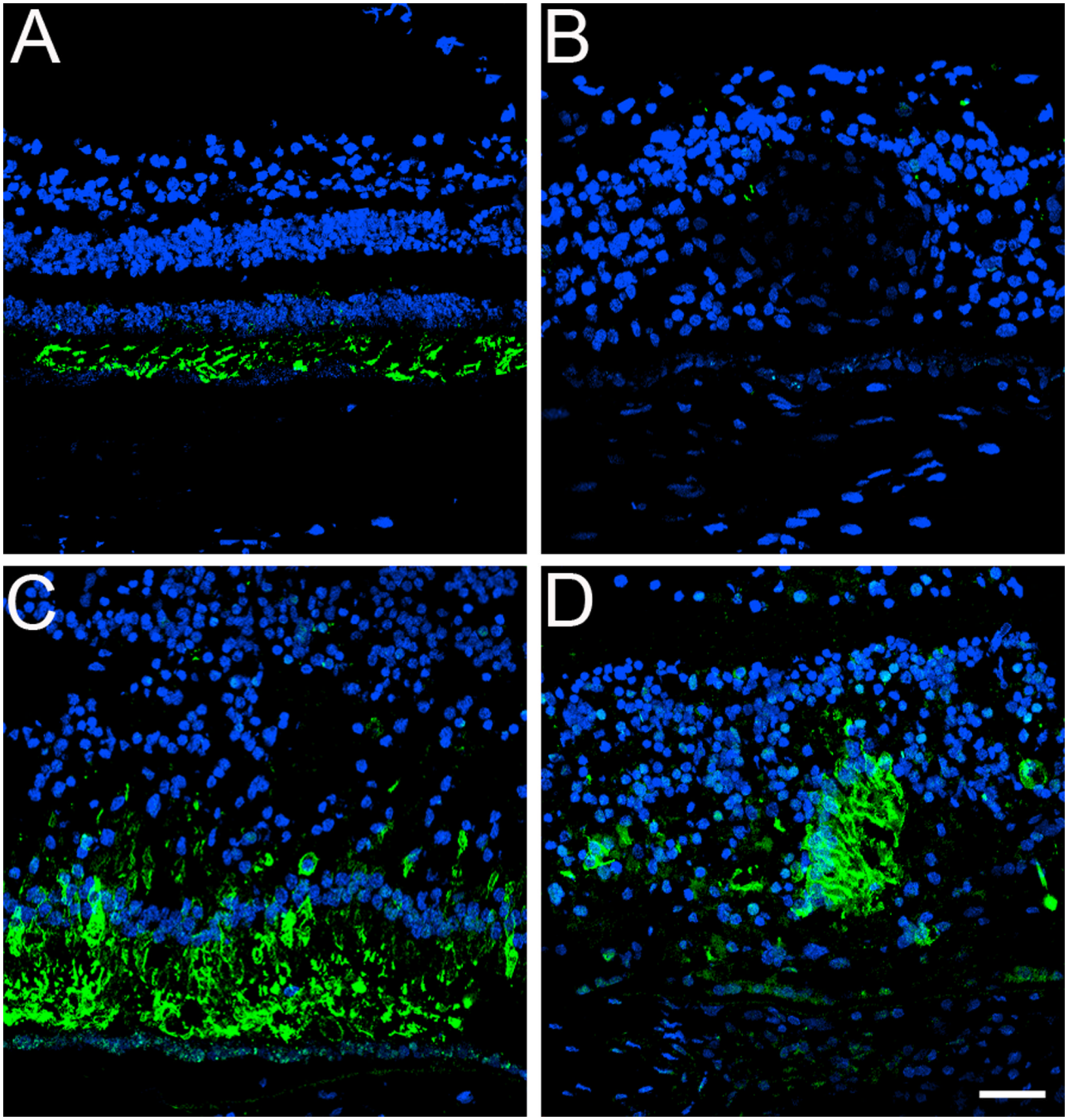


**Fig. 4.**

Red/green cone opsin is distributed along the entire plasma membrane of this cone type in a GFS affected donor. Human cryosections of both a matched control (A) and affected GFS donor (B-D) were labeled with antibodies specific to red/green cone opsins (Alexa488, green) while cell nuclei were labeled with TO-PRO-3 (blue). Sections were analyzed using a Leica laser scanning confocal microscope. Comparison of the samples showed that red/green cone opsins were distributed along the entire plasma membrane of this cone type in the perimacular region (C, D); this abnormal distribution was also observed in rosettes in a perimacular location (D). On the other hand, red/green opsins were mostly absent in the periphery of the affected retina (B). Scale bar = 40μm.

NIH-PA Author Manuscript
NIH-PA Author Manuscript
NIH-PA Author Manuscript



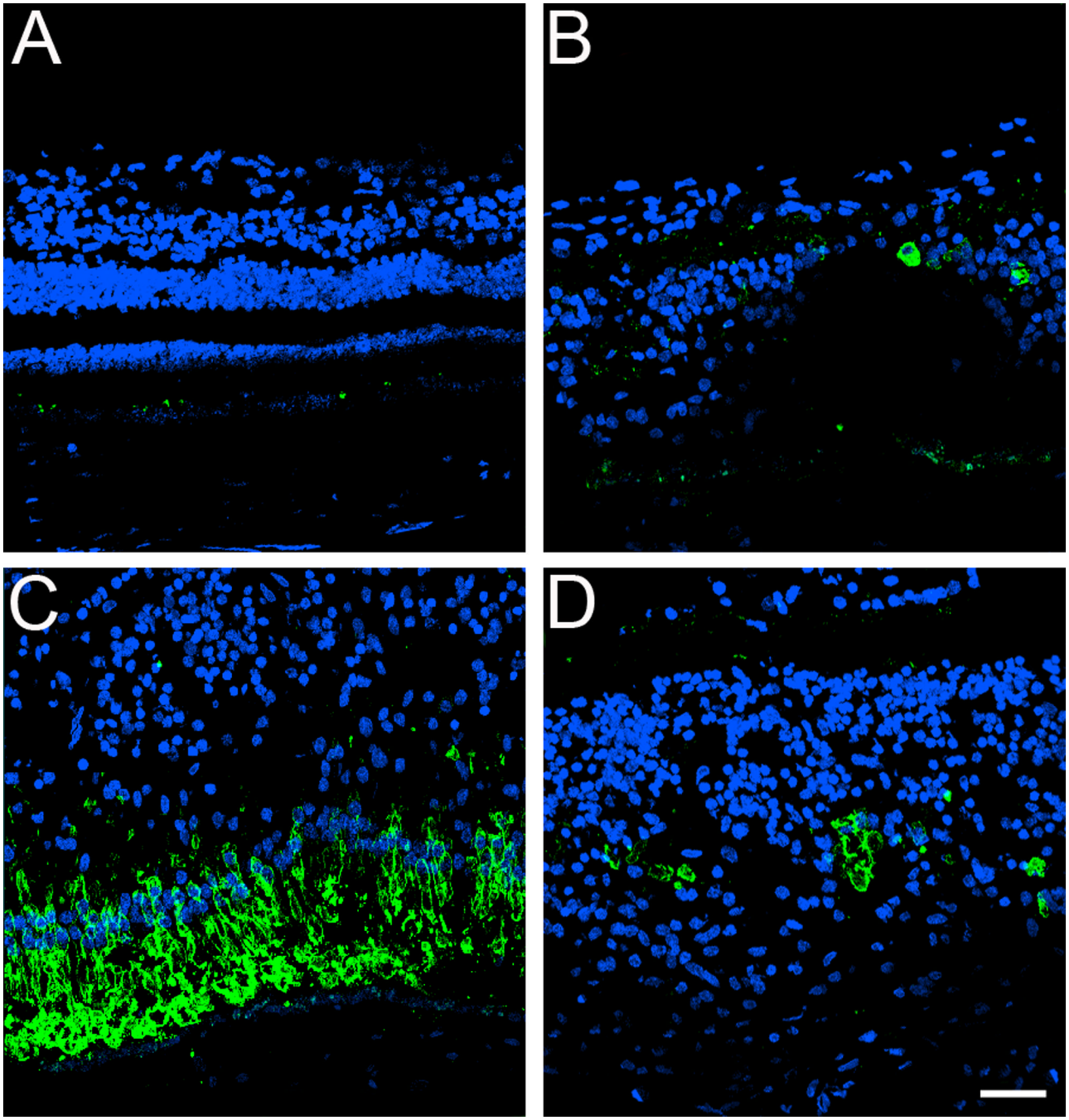


**Fig. 5.**

Blue cone opsin is significantly increased and distributed along the entire plasma membrane of this cone type in a GFS affected donor. Human cryosections of both a matched control (A) and affected GFS donor (B–D) were labeled with antibodies specific to blue cone opsins (Alexa488, green) while cell nuclei were labeled with TO-PRO-3 (blue). Sections were analyzed using a Leica laser scanning confocal microscope. Comparison of the samples showed that blue cone opsins were significantly increased both in the periphery (B) and perimacular region (C, D) of the affected eye, where blue cone opsins were distributed along the entire plasma membrane of this cone type; the abnormal distribution was also observed in rosettes in a perimacular location (D). Scale bar = 40μm.

NIH-PA Author Manuscript
NIH-PA Author Manuscript
NIH-PA Author Manuscript



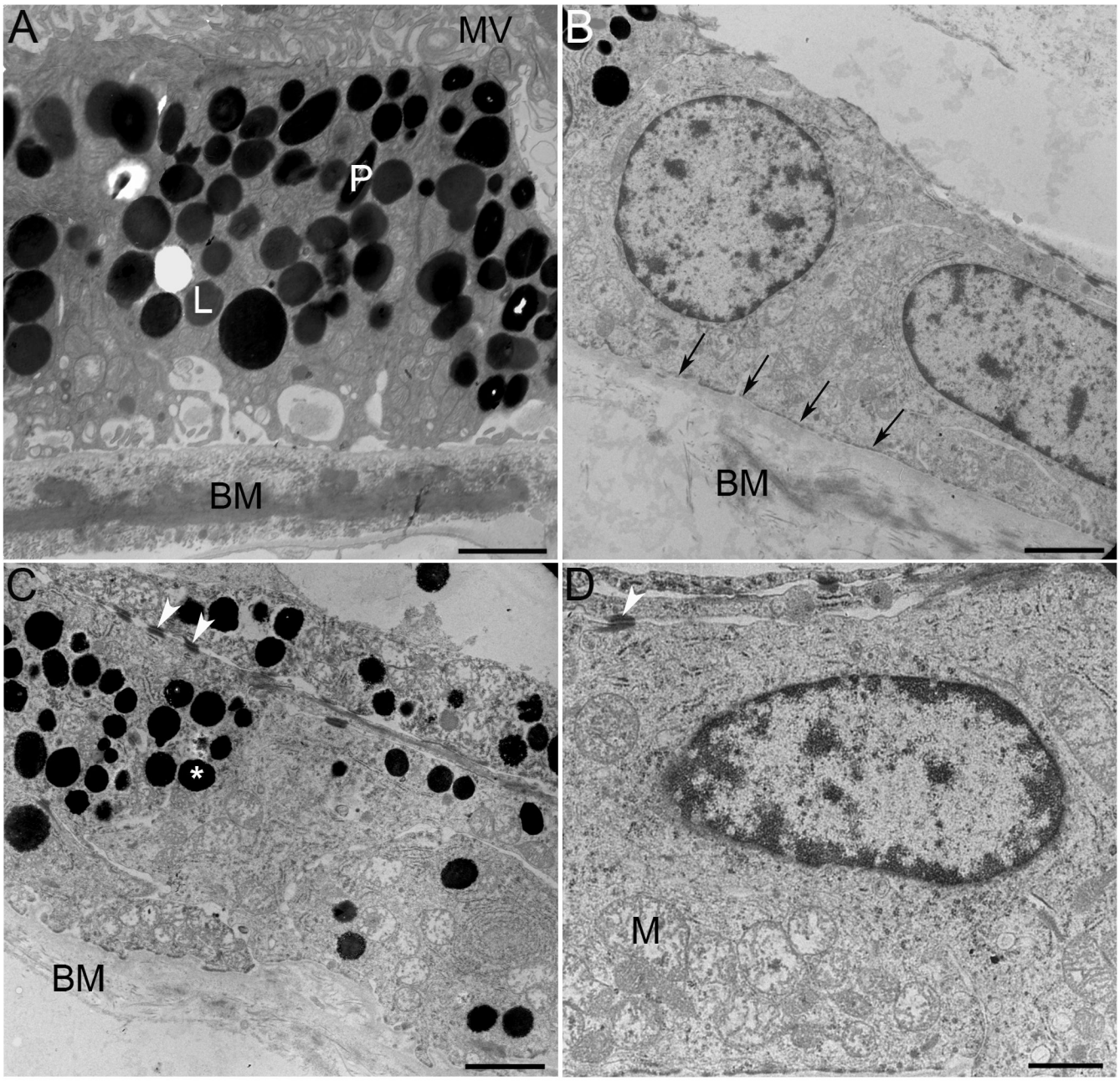


**Fig. 6.**

Ultrastructural evidence of RPE degeneration in a GFS affected donor. The ultrastructure of perimacular tissue was analyzed by TEM. Observation at both low (B, C) and high (D) magnification showed a collapsed RPE apical surface mostly deprived of apical microvilli; no photoreceptor outer segments are observed on top of the RPE apical surface. Moreover, observation of RPE's basal surface showed absence of basal infoldings (arrows); Bruch's membrane was very disorganized (B, C) when compared to control sample (A). Some areas displayed multilayers of pigmented cells (C). The presence of desmosomes (C, D, arrowheads) was noticed between adjacent cells. The cytoplasm of RPE cells was filled with abnormally large (>1mm) spherical electrondense melanosomes (B, C, *) when compared to a control RPE cell (A). Electron micrographs were taken on a Tecnai 20, 200 kv digital

electron microscope using a Gatan image filter. N= nucleus; M= mitochondria; MV= microvilli; BM= Bruch's membrane; L= lipofuscin granules; P=pigment. Scale bars: A, B, C = 2μm and D =1μm.

NIH-PA Author Manuscript
NIH-PA Author Manuscript
NIH-PA Author Manuscript